

## SURROGATE MODELING TECHNIQUE FOR THE CONCEPTUAL AND PRELIMINARY DESIGN OF EMBEDDED ACTUATION SYSTEMS AND COMPONENTS

**Florian Sanchez\* Scott Delbecq\*\***

**\*Institut Clément Ader, UMR CNRS 5312, Paul Sabatier University, Toulouse**

**\*\* Institut Clément Ader, UMR CNRS 5312, Safran Electronics & Defense, Massy**

**Keywords:** *Surrogate modeling, Preliminary design, Electromechanical actuator, Multi-Disciplinary Optimization, Model-Based Design*

### Abstract

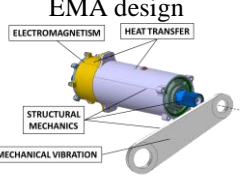
This paper presents a surrogate modelling technique adapted to multidisciplinary optimization problems involved during preliminary design and sizing of actuation systems and components. The proposed methodology combines dimensional analysis and surrogate modelling technique to build light models from finite element simulations. The proposed methodology is applied here on an electromechanical actuator to build several components models. Then they are used in a case study for the sizing of an aileron rotary actuator.

### 1 Introduction

A lot of aircraft systems shift to new technologies and become more complex with new functions, new domains, and new components while having to be less costly, less bulky and more ecological. Electromechanical actuation (EMA) systems are an example of this technological evolution. These systems are multi-domain systems therefore their development requires multi-disciplinary techniques. As embedded system, the challenge is to design them as lightweight and as reliable as possible. Multidisciplinary optimization (MDO) is widely used for shape, topology or structural optimization as wing design [1] but less for actuation system design. In the first case, the problem concerns a large number of parameters following a restricted number of complex and strongly coupled physics. In the second case, the number of parameters and the physical laws describing the behavior of the system are various due to the number and

different technological domains of system's components. The main particularity is that these laws are strongly correlated through design process but less during CFD or FEM simulations. The Table 1 summarizes the main differences between MDO problems for wing design and MDO problems for system design. The large number of interactions between different physical domains makes actuation system design close to aircraft design.

**Table 1: Comparison between MDO for wing design and MDO for system design**

	MDO for aero & structural design	MDO for system design
Example	 <p>Wing design STRUCTURAL, CFD</p>	 <p>EMA design ELECTROMAGNETISM, HEAT TRANSFER, STRUCTURAL MECHANICS, MECHANICAL VIBRATION</p>
Variables	Large number due to structural and shape variables	Large number due to number of components and design scenarios
Simulation models type	CFD and FEM	CFD, FEM but also lumped parameter models
Domains	Mainly fluid and structural physical domains	Structural mechanics, electromagnetism, heat transfer, control, etc.
Domains coupling	Strongly coupled	Weakly coupled
Design criterion types	Large number due to high complexity of models	Large number due to different technology of components and system sizing scenarios

The methodology proposed here is a solution for representing CFD or FEM component models for system design that requires MDO.

After a short introduction of the theoretical concepts used, the different steps of the proposed methodology are described. Then the methodology is applied to the electromechanical actuator of an aileron in order to build several models necessary for its preliminary design. At the end a multi-disciplinary optimization procedure is conducted to design the actuator.

## 2 Surrogate modeling technique: the Variable Power Law Metamodel (VPLM) methodology

### 2.1 Dimensional analysis & surrogate modeling technique

Surrogate modelling with dimensional analysis is an alternative school to build surrogate models that rely more on physical reasoning than on mathematical approaches. The reader can follow the references [2,3] to become more familiar with surrogate modelling techniques. Dimensional analysis is a powerful way to get there and is mainly based on the Buckingham theorem [4]. The following equation is the classical mathematical representation of a physical problem involved in component selection when surrogate modelling approach is used:

$$y = f(\underbrace{d_1, d_2, \dots, p_1, p_2, \dots}_n) \quad (1)$$

where:

- $y$  is the physical characteristic of a component which is useful for its selection in a system, such as the thermal resistance or the electromagnetic torque of a motor.
- $d_i$  are the geometrical dimensions of the component. These dimensions may vary on large intervals during global system design.
- $p_i$  are boundary conditions or material properties used in the design of the components.

It is important to note that  $d_i$  and  $p_i$  are  $n$  independent variables and  $y$  is a dependent variable.

Using dimensional analysis principle, equation (1) can be rewritten in the form:

$$\pi_0 = F\left(\underbrace{\pi_1, \pi_2, \dots, \pi_q}_q\right) \quad (2)$$

Where:

- $\pi_i$  are dimensionless variables, also called dimensionless numbers
- $q$  is the number of dimensionless numbers, which is function of the  $m$  independent physical units (e.g. m, kg, s, etc.) and the  $n$  variables involved in the problem. It is calculated using the relationship:  $q = n - m$ .

The output response  $y$  is also modified in order to become dimensionless:

$$\pi_0 = y \prod_{i=1}^q d_i^{a_i} p_i^{b_i} \quad (3)$$

This classical approach in fluid mechanics and heat transfer [5] is used in other different domains and uses different mathematical forms (Table 2). The methodology proposed here uses also this approach with an original mathematical form of model.

**Table 2: Synthesis of mathematical forms used in Dimensional Analysis based approaches**

Approaches	Mathematical form of the model	Eq. ref.	Lit. ref.
Power laws with $\pi_i$ numbers	$\pi_0 = a_0 \prod_{i=1}^q \pi_i^{a_i}$	(4)	[5]
SLAW method: Power laws with $d_i$ & $p_i$ numbers	$y = a_0 \prod_{i=1}^n d_i^{a_i} p_i^{b_i}$	(5)	[6]
Scaling laws	$y = kL^a$	(6)	[7,8]
Scaling laws meta-models (SLAWMM)	$y = f(L, \pi_1, \pi_2, \dots) = k(\pi_1, \pi_2, \dots) L^{a(\pi_1, \pi_2, \dots)}$ with $\pi_i = \frac{d_i}{L}$	(7)	[9,10]
Polynomial meta-models with $\pi_i$ numbers	$\pi_0 = a_0 + \sum_{i=1}^q a_i \pi_i + \sum_{i=1}^q a_{ii} \pi_i^2 + \sum_{i=1}^q \sum_{j=1}^i a_{ij} \pi_i \pi_j$	(8)	[11–13]
Sum of power law meta-model	$\pi_0 = \sum_{j=1}^m \beta_{0j} \prod_{i=1}^q \pi_i^{\beta_{ij}}$	(9)	[14]

### 2.2 VPLM: Variable Power Law Meta-model

The methodology presented here is called Variable Power Law Meta-model (VPLM). It is

applied in four main steps: data generation, surrogate model definition, surrogate model selection and surrogate model optimization. Fig. 1 shows the global process of the methodology by presenting all the processes involved in each main step.

This methodology aims at facilitating the design of multi-physics systems and components by building surrogate models based on dimensional analysis and finite elements simulations.

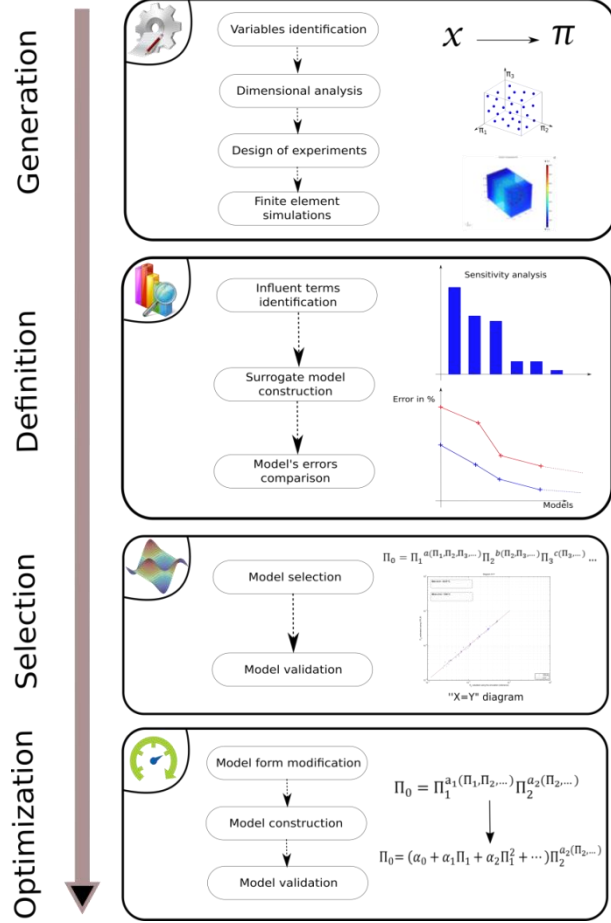


**Fig. 1: Procedure of the VPLM methodology**

### Data generation

This step is composed of four operations. The first one deals with the identification of the influent physical variables and the construction of the corresponding dimensionless numbers. More details on dimensional analysis can be found in [15]. Afterwards a DoE is established to define the configurations which have to be simulated in finite element simulation software.

### Surrogate model definition

This second step deals with the definition of the surrogate model, or in other words the algebraic expression of the model. As states the name of

the methodology (VPLM), the mathematical form of the chosen function is a variable power law. This choice was motivated by different observations and studies of the state of the art concerning the approximation models used in engineering. Although polynomial models are often used to build response surface models, a lot of engineering problems follow a power law behavior. In addition, for heat transfer problems the most used correlations to estimate the heat transfer coefficient are power law functions [5]. Regarding these observations, the most appropriate surrogate model form may be:

$$\pi_0 = k \pi_1^{a_1} \pi_2^{a_2} \dots \pi_n^{a_n} \quad (10)$$

where  $\pi_0$  is the dimensionless number containing the output,  $k$  and  $a_i$  are numerical coefficients and  $\pi_i$  are dimensionless numbers.

The relation (10) re-written in logarithmic scale corresponds to a response surface model of the first order:

$$\log(\pi_0) = \log(k) + \sum_{i=1}^q a_i \log(\pi_i) \quad (11)$$

However the literature review on correlation laws used in heat transfer shows that power law functions of dimensionless numbers do not represent all the configurations generally encountered [5]. Very often, the authors provide charts or tables with numerical values to be used for  $k$  and  $a_i$  depending on the value of dimensionless numbers. Thus, since engineers propose to increase the order of a polynomial model when its accuracy is not sufficient [16], we propose to increase the order of the model in equation (11). In order to keep simple the algebraic model, the VPLM methodology will estimate at most third order models. Thus, the general form of the proposed model is:

$$\begin{aligned} \log(\pi_0) = & \log(k) + \sum_{i=1}^q a_i \log(\pi_i) \\ & + \sum_{i=1}^q \sum_{j=1}^q b_{ij} \log(\pi_i) \log(\pi_j) \\ & + \sum_{i=1}^q \sum_{j=1}^i \sum_{k=1}^j c_{ijk} \log(\pi_i) \log(\pi_j) \log(\pi_k) \end{aligned} \quad (12)$$

where  $k$ ,  $a_i$ ,  $b_{ij}$  and  $c_{ijk}$  are numerical coefficients. By rewriting the relation (12) in the

linear scale we obtain a variable power law model as:

$$\pi_0 = k \pi_1^{a_1(\pi_1, \pi_2, \dots, \pi_q)} \pi_2^{a_2(\pi_1, \pi_2, \dots, \pi_q)} \dots \pi_q^{a_q(\pi_1, \pi_2, \dots, \pi_q)} \quad (13)$$

where  $a_i(\pi_1, \dots, \pi_q)$  are polynomial functions of  $\log(\pi_i)$ .

Most of the time models do not need to keep all the higher order terms<sup>1</sup> in the equation (12). In order to identify which ones deserve to be kept, a sensitivity analysis is conducted using the simulation data coming from the first step. Then, they are sorted in order of their importance (Fig. 2) and automatically  $m$  models are calculated where for the  $i^{\text{th}}$  model,  $i \in (0, m - 1)$ , only the first  $i$  higher order terms from Fig. 2 are considered. Note that for  $i = 0$  the obtained model is identical to the one in equation (10). The models are built by minimizing the least square error between the model and the simulation data [16].

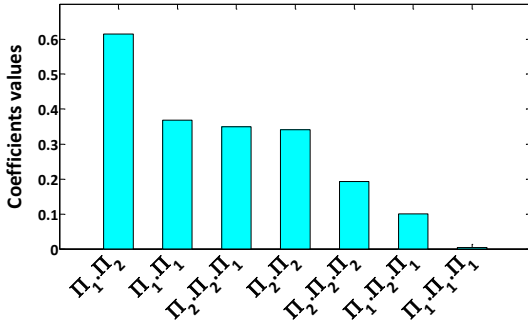


**Fig. 2: Example of higher order terms arrangement in function of their importance for the case of two dimensionless numbers**

### Surrogate model selection

This third step of the VPLM methodology concerns the selection of the appropriate model and its validation regarding its accuracy and complexity. During the previous step several candidate models were built and now we can evaluate the relative errors and/or the standard deviation for each one. In order to appreciate and compare the accuracy of the surrogate models built during the second step, the evolution of the relative errors of each model (differing in the number of selected higher order terms) are shown in Fig. 3. Thus the engineer

can make a compromise between accuracy and simplicity of the expected surrogate model.

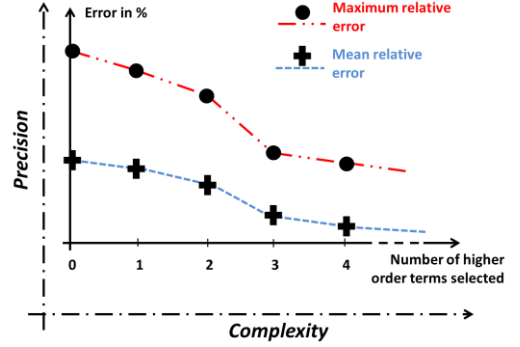


**Fig. 3: Example of relative errors comparison between different models**

Table 3 shows the evolution of VPLM models following the horizontal axis in Fig. 3, that corresponds to the arrangement of the terms from Fig. 2. Thus, by looking at Fig. 3 and Table 3 it can be seen that the prediction accuracy increases with the number of selected terms, but the model becomes more bulky as well.

**Table 3: Evolution of the VPLM models with the higher order terms selection**

Nb. of terms	Form of the VPLM model	
0	$\pi_0 = k \pi_1^{a_1} \pi_2^{a_2}$	(14)
1	$\pi_0 = k \pi_1^{a_1 + b_{12} \log(\pi_2)} \pi_2^{a_2}$	(15)
4	$\pi_0 = k \pi_1^{a_1 + b_{11} \log(\pi_1) + b_{12} \log(\pi_2)} \pi_2^{a_2 + b_{22} \log(\pi_2) + c_{221} \log(\pi_2) \log(\pi_1)}$	(16)

### Surrogate model form optimization

Even if many models involved in engineering problems follow power law behavior, in some cases this mathematical form may not give the expected accuracy. This step of the VPLM methodology gives the possibility to optimize the surrogate model form in order to achieve the expected accuracy.

## 3 Rotary electromechanical actuator models

### 3.1 EMA description

Nowadays, aircraft manufacturers express their interest for future wing concepts. Indeed, these innovative wing designs could increase overall

<sup>1</sup> Here, the higher order terms are those multiplied by  $b_{ij}$  and  $c_{ijk}$

aircraft's efficiency. Currently, flight control actuation systems do not meet the requirements brought by future wing concepts in terms of integration or thermal performances for instance.

As an answer to this challenge, equipment manufacturers must develop innovative actuator subsystems such as power electronics [17] or electromechanical units (EMU). To prepare the More Electrical Aircraft, Safran Electronics & Defense (former Sagem) has developed several EMAs. One of them is a primary flight control on-hinge rotary EMA.



**Fig. 4: FRACASS Rotary EMA [18]**

Using this relevant experience, models of existing components can be implemented. By combining these models and MDO it is possible to optimize and evaluate a specific actuator design. In this paper, the following aileron rotary actuator architecture will be studied.

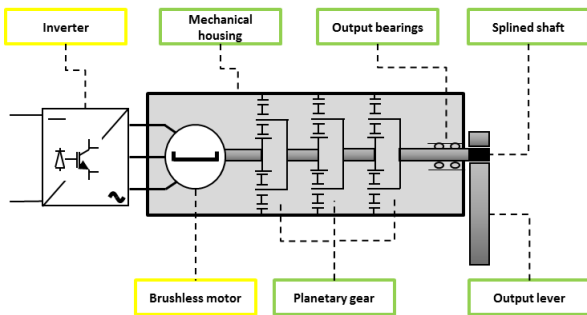


**Fig. 5: Actuator power architecture**

The objective of the study is to optimize the EMU (no inverter) overall design in terms of mass. For that, different type of models will be used.

The design of three stages planetary gear reducer, output bearings, housing (mechanical model) and splined shaft is done using scaling laws models. These models are built using similar methods described by [7] and use reference components developed by Safran Electronics & Defense for R&T projects.

The brushless motor, output lever and housing (thermal model) will be sized using surrogate model respecting VPLM methodology

developed at Institut Clément Ader. These models will be detailed in the following part.

### 3.2 Brushless motor models

#### 3.2.1 Electromagnetic model

In this study, the Parvex NX310 brushless motor serves as a reference because it is similar to the ones used in aerospace applications, in terms of dimensions and performance. Its interior is illustrated in Fig. 6. A Safran Electronics & Defense motor would have been wiser for aileron application because of its damping characteristic. Indeed, it helps avoid flutter at surface level but it is not used in this study for confidentiality reasons.

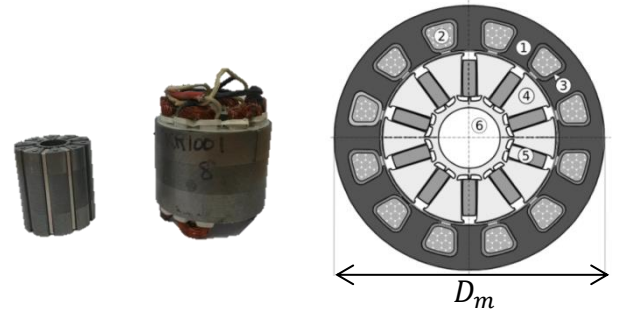


**Fig. 6: PARVEX NX310 (left), Sectional view of Parvex NX310 (right)**

**Table 4: Material used for the brushless motor model**

Ref.	1, 4	2	3	5	6
Material	Iron	Copper - Resin	Nomex	SmCo	Air

The electromagnetic domain is characterised by nine physical quantities:

$$T_m/L = f(D_m, J, B_r, B_{sat}, \mu_0, e_{air}, e_{Nomex}) \quad (17)$$

where  $T_m/L$  is the linear torque,  $D_m$  the diameter,  $J$  the current density,  $B_r$  the remanent induction of permanent magnets,  $B_{sat}$  saturation induction of iron sheet,  $\mu_0$  permeability of vacuum,  $e_{air}$  width of air gap between stator and rotor, and  $e_{Nomex}$  the thickness of Nomex insulation layers.

The Buckingham theorem modified by Sonin [19] led to the following dimensionless form:

$$\pi_{mag} = F(\pi_1, \pi_2, \pi_3) \quad (18)$$

Where  $\pi_{mag} = T_m/B_r J D_m^3 L$ ,  $\pi_1 = \mu_0 J D_m / B_{sat}$ ,  $\pi_2 = e_{air} / D_m$  and  $\pi_3 = e_{Nomex} / D_m$ .

Following the VPLM methodology, a design of experiments of 50 points (Table 5) is built to

define the configurations simulated in Finite Element Methods Magnetics (FEMM).

**Table 5: Ranges for the variables of the brushless motor models**

Variables	Units	Ranges
$D_m$	mm	30 – 150
$J$	A/mm <sup>2</sup>	7 – 250
$\pi_1$	-	0.62 – 4.43
$\pi_2$	-	0.002 – 0.133
$\pi_3$	-	0.0026 – 0.0133

The VPLM methodology procedure associated with a polynomial combined with a power law as shape function (according the fourth step of the VPLM methodology), leads to a maximum relative error of 5.4%.

$T_m =$

$$B_r J D_m L_m \cdot (0.147 \pi_1^{-0.184} (0.0922 - 13.8 \pi_2 + 10.99 \pi_3 + 56.37 \pi_2^2 + 33.62 \pi_3^2 + 43.65 \pi_2 \pi_3)) \quad (19)$$

### 3.2.2 Thermal model (conduction)

The thermal model of the brushless electrical motor will permit to evaluate the thermal resistance  $R_{cd}$  which describes the heat transfer by conduction between the hotspot temperature of the motor  $\theta_{hot}$  and the temperature on the external surface of the motor  $\theta_{surf}$ . The problem depends on six physical variables:

$$R_{cd} = f(D_m, L_m, e_{Nomex}, \lambda_{iron}, \lambda_{mix}, \lambda_{Nomex}) \quad (20)$$

Where  $D_m$  is the diameter of the motor,  $L_m$  the length of the motor,  $e_{Nomex}$  the thickness of the Nomex paper (electrical insulation around each slot),  $\lambda_{iron}$  the thermal conductivity of iron,  $\lambda_{mix}$  the thermal conductivity of the mixture [20] and  $\lambda_{Nomex}$  the thermal conductivity of the Nomex. It is assumed here that all the material properties are constant. According to the modified form of the Buckingham theorem, only one dimensionless number is necessary to evaluate the thermal resistance  $R_{cd}$ :  $\pi_{cd} = f(\pi_3)$ . Where  $\pi_{cd} = \lambda_{iron} L_m R_{cd}$  and the dimensionless number  $\pi_3 = e_{Nomex}/D_m$  as defined for the electromagnetic model. A 2-D model is created in COMSOL Multiphysics and a design of experiments of 20 points is defined according to the range defined for  $\pi_3$  in the

Table 5. The selected surrogate model is the one with one higher order term (Fig. 7).

$$R_{cd} = \frac{317.7}{\lambda_{iron} L_m} \pi_3^{-1.57 + 0.25 \log(\pi_3)} \quad (21)$$

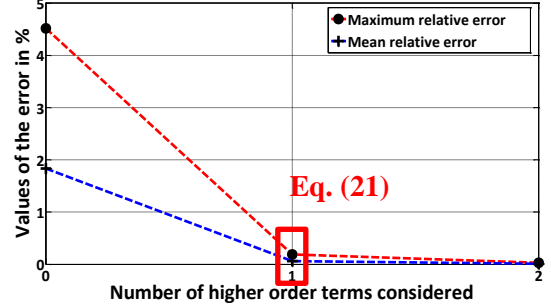


**Fig. 7: Evolution of the error of VPLM models for the motor thermal model**

### 3.3 Output lever models

This paragraph deals with the construction of the models necessary to perform the sizing of the output lever. Fig. 8 describes the geometrical configuration chosen. For the preliminary design of the output lever the important characteristics to be evaluated are: its mechanical stiffness  $K_r$ , its natural frequencies in flexion  $f_{r1}$  and  $f_{r2}$  and its admissible equivalent stress  $\sigma_r$ . It is proposed here to use the VPLM methodology to build the models to evaluate these mechanical characteristics of the output lever.

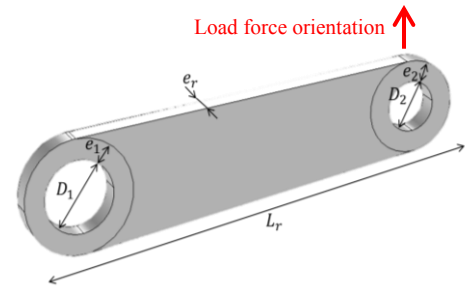


**Fig. 8: Geometrical configuration of the output lever**

#### 3.3.1 Stiffness model

The model built here will permit to evaluate the bending stiffness of the lever  $K_r$ . The output lever is clamped on one side, and on the other side a load force  $F$  is applied (Fig. 8). The problem depends on five physical variables:

$$K_r = f(E, D_1, D_2, L_r, e_r) \quad (22)$$

Where  $E$  is the Young modulus of steel,  $D_1$  and  $D_2$  are the diameters of the holes,  $L_r$  is the length of the lever and  $e_r$  is the thickness of the lever. For this study, the variables  $e_1$  and  $e_2$  are function of the diameters  $D_1$  and  $D_2$ :  $e_1 = D_1/4$ ,  $e_2 = D_2/4$ .

The modified form of the Buckingham theorem led to the following dimensionless form:

$$\pi_K = F(\pi_1, \pi_2, \pi_3) \quad (23)$$

Where  $\pi_K = \frac{K}{EL_r^3}$ ,  $\pi_1 = \frac{D_1}{L_r}$ ,  $\pi_2 = \frac{D_2}{L_r}$  and  $\pi_3 = \frac{e_r}{L_r}$ .

Following the VPLM methodology, a design of experiments of 64 points is built to define the configurations simulated in COMSOL Multiphysics. The Table 6 gives the ranges for all the variables used for the lever models.

**Table 6: Ranges for the variables of the output lever models**

Variables	Units	Ranges
$D_1$	mm	10 – 50
$D_2$	mm	10 – 50
$e_r$	mm	5 – 30
$L_r$	mm	150 – 300
$F$	N	4000 – 10000
$\pi_1$	-	0.03 – 0.33
$\pi_2$	-	0.03 – 0.33
$\pi_3$	-	0.016 – 0.33
$\pi_4$	-	$2.2 \cdot 10^{-7} - 2.2 \cdot 10^{-6}$

Fig. 9 shows that the model with 3 higher order terms gives the best compromise between accuracy and complexity.

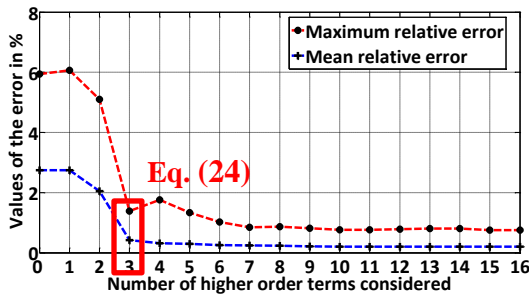


**Fig. 9: Evolution of the model's error for the stiffness model of the lever**

$$K_r = 2.138 EL_r^3 \pi_1^{2.5-0.236 \log(\pi_2)+0.197 \log(\pi_1)} \pi_2^{0.942+0.168 \log(\pi_2)} \pi_3 \quad (24)$$

### 3.3.2 Stress model

The model built here will permit to evaluate the equivalent stress due to bending of the lever  $\sigma_r$ .

The problem depends on five physical variables which are the geometrical parameters of the lever and the load  $F$ :

$$\sigma_r = f(D_1, D_2, L_r, e_r, F) \quad (25)$$

The modified form of the Buckingham theorem led to the following dimensionless form:

$$\pi_\sigma = F(\pi_1, \pi_2, \pi_3) \quad (26)$$

Where  $\pi_\sigma = \sigma_r / (F/L_r^2)$  and the dimensionless numbers  $\pi_1, \pi_2$  and  $\pi_3$  are the same already used for the stiffness model.

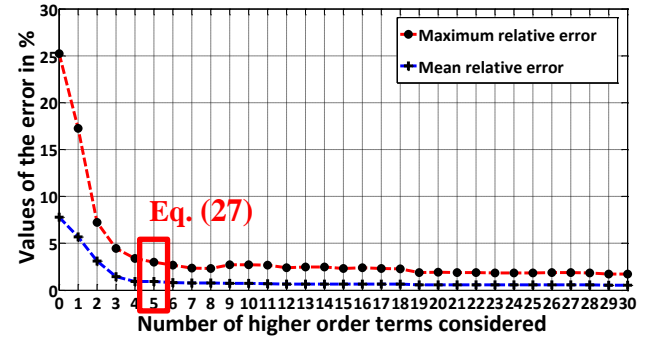


**Fig. 10: Evolution of the model's error for the stress model of the output lever**

$$\sigma_r = (0.123 F/L_r^2)$$

$$\pi_1^{-2.547-0.103 \log(\pi_2) \log(\pi_1)-0.252 \log(\pi_2) \log(\pi_2)} \pi_2^{-1.906-0.616 \log(\pi_2)-0.0435 \log(\pi_2) \log(\pi_2)-1.045 \log(\pi_1)} \pi_3^{-1} \quad (27)$$

### 3.3.3 Vibratory model

The model built here will permit to evaluate two bending natural frequencies of the output lever respecting the boundary conditions of the problem. The output lever is clamped on both sides. The problem depends on six physical variables which are the properties of steel and the geometrical parameters of the lever.

$$f_r = f(E, \rho, D_1, D_2, L_r, e_r) \quad (28)$$

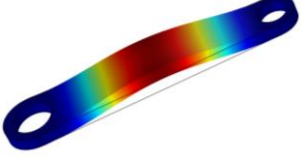
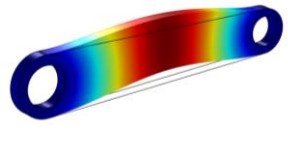
The modified form of the Buckingham theorem led to the following dimensionless form:

$$\pi_f = F(\pi_1, \pi_2, \pi_3) \quad (29)$$

Where  $\pi_f = f_r L_r (\rho/E)^{1/2}$  and  $\pi_1, \pi_2$  and  $\pi_3$  are the same dimensionless numbers used for the stiffness and stress models. The design of experiment used for the stiffness model is used to define the configurations simulated in COMSOL Multiphysics. Two different VPLM

models are built to evaluate two different bending natural frequencies (Table 7). The models (30) and (31) have a maximum error of 13% and 3% respectively.

**Table 7: Vibratory models for the lever**

Natural frequency in transverse bending (30)	Natural frequency in normal bending (31)
	
$f_{r1} = \frac{26.086}{L_r} \left(\frac{E}{\rho}\right)^{1/2} \pi_1^{2.872+1.895 \log(\pi_1)+0.462 \log(\pi_1) \log(\pi_1)} \pi_2^{0.856+0.373 \log(\pi_2)} \pi_3^{0.926}$	(30)
$f_{r2} = \frac{14.502}{L_r} \left(\frac{E}{\rho}\right)^{1/2} \pi_1^{1.534+1.028 \log(\pi_1)+0.244 \log(\pi_1) \log(\pi_1)} \pi_2^{1.633+1.225 \log(\pi_2)+0.275 \log(\pi_2) \log(\pi_2)-0.341 \log(\pi_1)} \pi_3^{0.0019}$	(31)

### 3.4 EMA housing thermal model

The objective here is to build the thermal model of the EMA housing using the VPLM methodology. The thermal model will permit to evaluate the thermal resistance of the EMA housing regarding its environment of integration (Fig. 11). The assumptions are:

- The heat transfer through the housing extremities is not considered.
- Natural convection cooling is assumed.
- All the walls of the environment are assumed to be at the external temperature.
- The properties of air are assumed to be constant for the study and evaluated at the mean temperature.
- The size of the environment of integration of the EMA is constant.

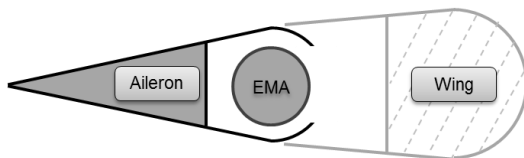


**Fig. 11: EMA aileron environment**

The thermal resistance of the EMA housing  $R_a$  depends on eight physical quantities:

$$R_{cv} = f(D_a, g\beta\Delta\theta, \rho, \mu, \lambda, C_p, Le, He) \quad (32)$$

Where  $D_a$  is the diameter of the housing,  $g\beta\Delta\theta$  represents the Archimedes' force due to the temperature difference between the housing and the environment,  $\rho$  is density of air,  $\mu$  is the dynamic viscosity of air,  $\lambda$  is the thermal conductivity of air,  $C_p$  is the heat capacity of air and  $Le, He$  define the size of the environment inside the wing. The Buckingham theorem modified by Sonin led to the following dimensionless form:

$$\pi_{cv} = F(Gr_{D_a}, \pi_2, \pi_3) \quad (33)$$

Where  $Gr_{D_a} = \rho^2 g\beta\phi D_a^4 / \lambda\mu^2$  is the Grashof number defined in terms of heat flux density  $\phi$ ,  $\pi_2 = Le/D_a$  and  $\pi_3 = He/D_a$  are geometrical ratios.

Following the VPLM methodology procedure, a design of experiments (Table 8) of 64 points is built to define the configurations simulated in COMSOL Multiphysics (Fig. 12).

**Table 8: Ranges for the DoE of the housing thermal model**

Variables	Units	Ranges
$D_a$	mm	50 – 100
$\phi$	W/mm <sup>2</sup>	500 – 2000
$Le$	mm	70 – 80
$Gr_{D_a}$	-	$4 \cdot 10^6 - 2.6 \cdot 10^8$
$\pi_2 = \frac{Le}{D_a}$	-	0.7 – 1.6
$\pi_3 = \frac{He}{D_a}$	-	1.2 – 2.4

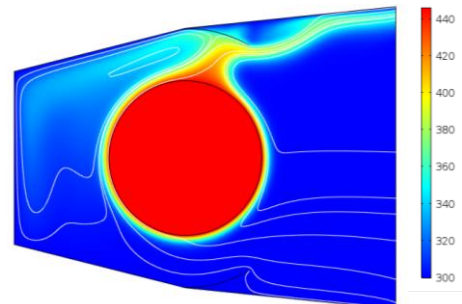


**Fig. 12: Temperature field [°K] for the natural convection cooling of the EMA**

The regression process led us to select the VPLM model with constant power coefficients

because it gives less than 3% of maximum relative error with the simplest mathematical expression.

$$R_{cv} = \frac{0.317}{\lambda D_a} \pi_2^{0.0177} \pi_3^{-1.121} Gr_{D_a}^{-0.194} \quad (34)$$

## 4 Multidisciplinary optimization of a rotary EMA

### 4.1.1 Problem statement

As described by the Figure 13, the components characteristics are strongly correlated to each other and to the sizing scenarios considered. In this paper we will consider only the red links which are involved in the presented models.

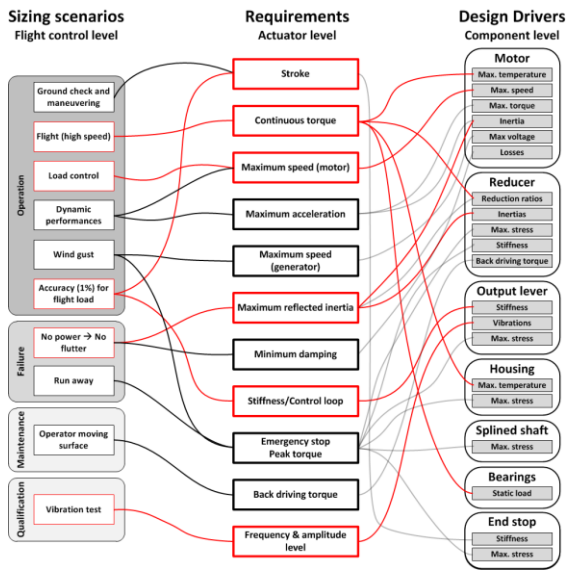


**Fig. 13: Aileron EMA main sizing scenarios**

By using a sizing model representing the system and choosing acute sizing variables, it is possible to obtain the design which leads to an optimized overall mass of the actuator. The problem is implemented and solved using the SLSQP optimizer within openMDAO. This Python framework offers an efficient structure for using gradient based optimization to solve MDO problems [21]. Indeed, thanks to this framework, VPLM and scaling laws models are implemented and stored. The models are then connected in order to build the overall system model and apply the optimization problem to it. The Figure 14 shows the optimization problem implemented for the EMA design.

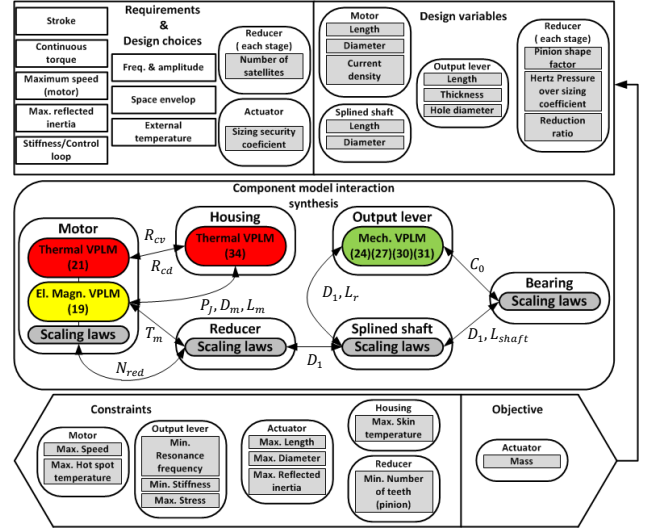


**Fig. 14: Optimization problem for the EMA preliminary design**

The use of meta-models and gradient based algorithms gives the possibility to find the optimized design within minutes.

### 4.1.2 Multidisciplinary optimization results

The results show that the active constraints are skin temperature and reflected inertia. Therefore to further increase mass gain, the actuator's thermal resistance has to be diminished or some work has to be conducted on the reflected inertia. Indeed, the actuator's reflected inertia may be reduced by changing the motor's technology or by increasing the cooling efficiency of the actuator. Thanks to sensitivity analysis of actuator design to requirements, another option is to renegotiate the reflected inertia requirement by quantifying mass gain for a given requirement change.

## 5 Conclusion

It has been shown here the possibility to create meta-models from FEM or CFD simulations representative of components main design drivers. Their association demonstrates their use during system early design stage. Their use increases the accuracy of the overall system parametric model, and consequently enables more realistic representation of sizing scenarios. Such parametric model and optimization tool gives the possibility to involve the supplier earlier in the aircraft development process for installation trade-off studies for instance. Furthermore, it reduces iterations between airframers and equipment or system suppliers during the preliminary design process.

**Nomenclature**

Acronym	
EMA	Electro-Mechanical Actuator
DoE	Design of Experiments
VPLM	Variable Power Law Meta-model
MDO	Multi-Disciplinary Optimization
EMU	Electro-Mechanical Unit
CFD	Computational Fluid Dynamics
Indices	
<i>a</i>	Actuator
<i>cd</i>	Conduction
<i>cv</i>	Convection
<i>m</i>	Motor
<i>mag</i>	Magnetic
<i>r</i>	Output lever
<i>sat</i>	Saturation

**References**

[1] Z. Lyu, J.R.R.A. Martins, Aerodynamic Shape Optimization of an Adaptive Morphing Trailing-Edge Wing, *J. Aircr.* 52 (2015) 1951–1970. doi:10.2514/1.C033116.

[2] A.I.J. Forrester, A. Sóbester, A.J. Keane, *Engineering Design via Surrogate Modelling*, 2008.

[3] T.W. Simpson, J.D. Peplinski, P.N. Koch, J.K. Allen, *Metamodels for Computer-based Engineering Design : Survey and recommendations*, (2001) 129–150.

[4] E. Buckingham, On physically similar systems: illustration of the use of dimensional equations, *Phys. Rev.* 4 (1914) 345–376.

[5] F.P. Incropera, D.P. DeWitt, T.L. Bergman, A.S. Lavine, *Fundamentals of Heat and Mass Transfer*, John Wiley & Sons, 2007. [http://www.osti.gov/energycitations/product.biblio.jsp?osti\\_id=6008324](http://www.osti.gov/energycitations/product.biblio.jsp?osti_id=6008324).

[6] P.F. Mendez, F. Ordóñez, *Scaling Laws From Statistical Data and Dimensional Analysis*, *J. Appl. Mech.* 72 (2005) 648. doi:10.1115/1.1943434.

[7] M. Budinger, J. Liscouet, F. Hospital, J.-C. Mare, Estimation models for the preliminary design of electromechanical actuators, *Proc. Inst. Mech. Eng. Part G J. Aerosp. Eng.* 226 (2011) 243–259. doi:10.1177/0954410011408941.

[8] M. Pfennig, U.B. Carl, F. Thielecke, Recent Advances Towards an Integrated and Optimized Design of High Lift Actuation Systems, *SAE Int. J. Aerosp.* 3 (2009) 2009–01–3217. doi:10.4271/2009-01-3217.

[9] M. Budinger, J.-C. Passieux, C. Gogu, A. Fraj, Scaling-law-based metamodels for the sizing of mechatronic systems, *Mechatronics*. (2013). doi:10.1016/j.mechatronics.2013.11.012.

[10] I. Hazyuk, M. Budinger, F. Sanchez, J.-C. Maré, S. Colin, Scaling laws based metamodels for the selection of the cooling strategy of electromechanical actuators in the early design

stages, *Mechatronics*. (2015). doi:10.1016/j.mechatronics.2015.05.011.

[11] D. Lacey, C. Steele, The use of dimensional analysis to augment design of experiments for optimization and robustification, *J. Eng. Des.* 17 (2006) 55–73. doi:10.1080/09544820500275594.

[12] G.A. Vignaux, J.L. Scott, Simplifying regression models using dimensional analysis, *Austral. New Zeal. J. Stat.* 41 (1999) 31–41.

[13] C. Gogu, R.T. Haftka, S.K. Bapanapalli, B. V. Sankar, Dimensionality Reduction Approach for Response Surface Approximations: Application to Thermal Design, *AIAA J.* 47 (2009) 1700–1708. doi:10.2514/1.41414.

[14] C.-C. Li, Y.-C. Lee, A statistical procedure for model building in dimensional analysis, *Int. J. Heat Mass Transf.* 33 (1990) 1566–1567.

[15] T. Szirtes, P. Rózsa, *Applied Dimensional Analysis and Modeling*, 2007. doi:10.1016/B978-012370620-1.50023-X.

[16] J.A. Cornell, *Response surfaces: design and analyses*, Marcel Dekker, New York, 1987.

[17] J. Derrien, J.-C. Minichetti, E. Bridot, M. Wendling, Innovative Flight Control Systems Electronic Architectures for a More Electrical Aircraft, in: J.-C. Maré (Ed.), *Recent Adv. Aerosp. Actuation Syst. Components*, INSA Toulouse, Toulouse, 2014: pp. 35–42.

[18] A. Sassier, H. Gadant, L. Baxerres, M. Todeschi, On Hinge Rotary Electro Mechanical Actuator development for primary flight control surfaces, in: *Symp. More Electr. Aircr.*, Toulouse, 2015.

[19] A.A. Sonin, A generalization of the PI-theorem and dimensional analysis, *Proc. Natl. Acad. Sci. USA.* 101 (2004) 8525–8526.

[20] I. Laid, M. Xavier, B. Frédéric, B. Laurent, H. Emmanuel, Thermal Model With Winding Homogenization and FIT Discretization for Stator Slot, *IEEE.* 47 (2011) 4822–4826.

[21] J.S. Gray, J. Chin, T. Hearn, E.S. Hendricks, T.M. Lavelle, J. Martins, Thermodynamics For Gas Turbine Cycles With Analytic Derivatives in OpenMDAO, 57th AIAA/ASCE/AHS/ASC Struct. Struct. Dyn. Mater. Conf. (2016) 1–21. doi:10.2514/6.2016-0669.

**Contact Authors Email Address**

mailto:florian.sanchez@insa-toulouse.fr

mailto:scott.delbecq@safrangroup.com

**Copyright Statement**

The authors confirm that they, and/or their company or organization, hold copyright on all of the original material included in this paper. The authors also confirm that they have obtained permission, from the copyright holder of any third party material included in this paper, to publish it as part of their paper. The authors confirm that they give permission, or have obtained permission from the copyright holder of this paper, for the publication and distribution of this paper as part of the ICAS proceedings or as individual off-prints from the proceedings.